

## ORIGINAL RESEARCH ARTICLE

## Geographical Disparities in Pyrolysis-Induced Porosity of Activated Carbon from *Cocos nucifera* in Nigeria: A Comparative Analysis Across Political Regions

Ajibade I. I.<sup>1</sup>  and Maduka N. C.<sup>2</sup> <sup>1,2</sup>Department of Physics, Federal University Gusau, Nigeria**ABSTRACT**

There is an urgent and growing need for high-power energy sources due to the quick growth of portable electronic devices and hybrid electric cars. It is necessary to reevaluate biomass pyrolysis's ability to slow climate change. In the current work, African tall *Cocos nucifera* (CN) from Nigeria's three geo-political zones is chemically ground and pyrolyzed. The ground samples were washed with sulfuric acid to destroy the resistant lignin and the polymers with different activation temperatures (650–850°C) in the LT furnace. Through the use of Fourier Transform Infrared (FTIR), X-ray diffraction (XRD), RAMAN, and Field Emission Scanned Electromagnetic Microscopy (FESEM), and Brunauer–Emmett–Teller (BET), the molecular, physical, morphological, and porosimetry tests of the produced activated carbon were analysed. We found out that the surface area of samples with Relative Humidity (RH) within the range (of 65-85)% increases with increasing pyrolysis temperature, while those with lower (RH) have the highest surface area at 750°C. This implies that moisture content, a derivative of (RH), plays a significant role in the pyrolysis process, thereby aiding the mechanical strength of activated carbon for onward use in energy storage systems.

**ARTICLE HISTORY**

Received March 03, 2024

Accepted June 20, 2024

Published July 11, 2024

**KEYWORDS**

Biomass; chemical pulverization; energy density; lignin; polymers.



© The authors. This is an Open Access article distributed under the terms of the Creative Commons Attribution 4.0 License (<http://creativecommons.org/licenses/by/4.0>)

**INTRODUCTION**

Plant residues and agricultural wastes are major environmental concerns on a global scale since they are a contributing factor to the increase in greenhouse gas emissions. As a result, these agricultural wastes have been used by numerous researchers in a variety of ways, such as soil conditioning, soil remediation, waste management, mitigating the effects of climate change, carbon sequestration, catalysis, producing activated carbon using particular materials, and producing energy storage (Ulusal et al., 2021).

Activated carbons are widely used in many industrial applications because of their highly developed pore structures and large internal surface area. Over the previous few decades, these technologies have included those for gas purification, the removal of organic contaminants from water (such as drinking water and wastewater purification), the use of these materials as electrode materials in electrochemical devices and processes, and the use of these materials as a catalyst or catalyst support in catalytic processes (Ajien et al., 2023). Hence, activated carbon has become extremely important to the food, drug, and chemical industries. Despite being the initial absorbent identified and maintaining its widespread use in industry, the evolution of suitable manufacturing methods and the exploration of its porous

structure persist (Lan et al., 2023). The preparation of activated carbons is widely acknowledged to involve various precursors characterized by a high carbon content and minimal inorganic compound levels (Hasdi et al., 2023). Scholarly literature documents that the nature of the precursor, the activation method, and the activation conditions affect the porosity properties in activated carbons, including pore size distribution, pore morphologies, and surface chemistry. Scholarly literature documents that the nature of the precursor, the activation method, and the activation conditions affect the porosity properties in activated carbons, including pore size distribution, pore morphologies,

and surface chemistry (Oglou et al., 2023). Various pore structures in activated carbons can be generated from a common precursor by adjusting the operational parameters and activation agent. While coconut shells have proven effective in producing activated carbons, there is limited information on their utilization in chemical activation. In particular, there hasn't been a thorough investigation into how the carbonization temperature affects the porosity properties of activated carbon made from coconut shells from various Nigerian provinces. Improving the carbon content and creating early porosity in the char are the main goals of the carbonization

**Correspondence:** Ajibade I. I. Department of Physics, Federal University Gusau, Nigeria. ✉ [isaajibade@fugusau.edu.ng](mailto:isaajibade@fugusau.edu.ng).

**How to cite:** Ajibade, I. I., & Maduka, N. C. (2024). Geographical Disparities in Pyrolysis-Induced Porosity of Activated Carbon from *Cocos nucifera* in Nigeria: A Comparative Analysis Across Political Regions. *UMYU Scientifica*, 3(3), 45 – 54. <https://doi.org/10.56919/usci.2433.006>

process. A number of critical factors, such as the temperature at which carbonization occurs, are critical to creating activated carbon and impacting its overall structure. Research shows that higher carbonization temperatures cause a significant amount of volatiles to be released from the raw material, affecting porosity and product output. Compared to activated carbon samples from carbonized chars produced at lower carbonization temperatures, those made from carbonized chars obtained at higher temperatures had a larger micropore (Quan et al., 2021). It is possible to control and anticipate the type and amount of porosity in activated carbons by understanding the process of porosity development. Consequently, this makes it easier to manage and forecast how well they will function in different applications (Zhu et al., 2021).

Despite all these landmark achievements, super capacitor has numerous challenges varying from Ohmic leakage, self-discharged, charge distribution, mass loading, temperature dependent, matched application, electrolyte optimization, material selection, and pore structure Babu (2024). The performance of supercapacitors strongly depends on the morphology of the electrode materials, current collectors, electrolytes, and separators (Ghafoor et al., 2024). In particular, the morphology of the electrodes is crucial since the amount of charge stored is proportional to the effective surface area of the carbon material Platek-Mielczarek et al. (2024). An ideal electrode material is expected to exhibit high surface area, high porosity, homogeneous pore size distribution, high electrical conductivity, and low production costs (Zhang et al., 2024). Consequently, there is a need to consider factors such as the moisture level, which is influenced by relative humidity, as well as the age and type of coconut shells, which is crucial when evaluating the potential suitability of coconut shells as a raw material for producing activated carbon. This is especially important when considering their use in the creation of supercapacitors.

This study's main goal was to investigate the effects of varying pyrolysis temperatures on the porosity properties of carbonized coconut shell chars and the activated carbons that were subsequently produced from both high and low-humidity samples. The impact of pyrolysis temperature on the yields of carbonized coconut shell chars and the ensuing activated carbons was methodically evaluated in this study. Furthermore, the study examined the systematic impacts on pore formation in low-moisture-derived activated carbon and high-moisture coconut shells.

## MATERIALS AND METHOD

### Activated Carbon Preparation

The carbons that were activated (ACs) were made from coconut shell (CS) as follows; the CS was obtained from three geo-political zones in Nigeria with the following

geographical locations SW(6.52°N&3.38°E), SE(6.46°N&7.61°E), and NW(12.94°N&5.23°E). After cleaning and sizing (to around 5 cm), the CS was dried for 24 hours at 800C in an oven. Using a 500 $\mu$  sieve, the dry materials were crushed and separated. 1MH<sub>2</sub>SO<sub>4</sub> was used as a chemical to functionalize the CS powder. After standing in a fume hood for 48 hours, the functionalized CS was cleaned with DI water until a pH of 6.5 was reached. After that, the sample was dried for eighteen hours at 1200 C in an electric oven. These six samples were heated to three (3) distinct temperatures in an argon

atmosphere in a furnace with a flow rate of 300 mL/min, ramped at 10 °C/min, and held for two hours before cooling in the same furnace. Yield is ascertained (Sahu et al., 2023). The first portion was activated at 650° C, and the second and third portions were heated at 750° C and 850° C, respectively.

### Methodology for Characterization of Pulverized Carbon

The following characteristics were found in activated carbon samples of CS that were collected at three distinct geo-political zones at three distinct activation temperatures: 650 °C, 750 °C, and 850 °C.

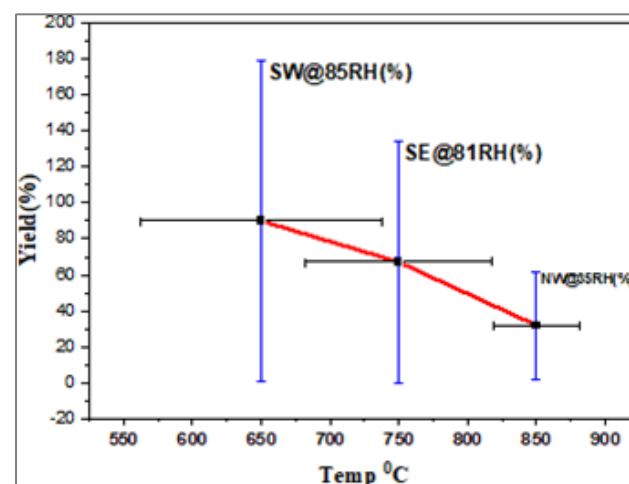


**Figure 1. Temperature and relative humidity during carbonization's impact on the yield of activated carbon from coconut shells.**

FTIR analysis (PerkinElmer Spectrum) using the traditional KBr approach was used to determine the presence of different functional groups within the sample in the 600–4000  $\text{cm}^{-1}$  range. X-ray diffraction (XRD) analysis was used to characterize the activated carbon products and examine their phase composition and crystallinity. Utilizing Co-K $\alpha$  radiation ( $\lambda = 1.79 \text{ \AA}$ ) and a BRUKER D8 ADVANCE X-RAY Diffractometer with a step size of 0.02° and a scan rate of 5°/min, the analysis was carried out in the 10–70° range. Analytical tools included a PL micro-Raman spectrometer (model XMB3000-3000) fitted with a 532 nm argon ion laser to determine whether ordered and disordered carbon was present in the activated carbon products. Field emission scanning was used to examine the surface morphology of

activated carbon from coconut shells. Field emission scanning electron microscopy (FESEM) analysis was performed using a FEI NOVANO SEM 450 instrument to investigate the surface morphology of activated carbon derived from Coconut shells. This analysis investigated samples prepared under different activation temperatures. Building on previous characterization methods, the investigation delved into the activated carbons' surface area and pore structure. This utilized nitrogen adsorption-desorption with a BET analyzer (Quanta chrome AUTOSORB-1) at  $-196^{\circ}\text{C}$  in liquid nitrogen. Before analysis, samples underwent degassing at  $200^{\circ}\text{C}$  for 6 hours to ensure accurate micropores, mesopores, total surface area, pore volume, and pore diameter measurements.

## RESULTS AND DISCUSSION

### The activated carbon's yield.

Yield refers to the ratio of the mass of activated carbon generated to the mass of the original material employed. The impact of activation temperature on the yield of each sample was examined. It was observed that with longer activation times, the yield percentage decreased, as illustrated in Figure 1. The yield of the activated carbons declined as the activation temperature rose from  $650^{\circ}\text{C}$  to  $750^{\circ}\text{C}$  and subsequently to  $850^{\circ}\text{C}$ , while the weight loss percentage increased. (Amin et al., 2023). A higher carbonization temperature causes more gasification reactions, which reduces yield. (Foo and Hameed 2012). The estimation of the carbon yield was calculated using Equation 2.

$$\text{Weight loss (\%)} = \frac{\text{Weight loss}}{\text{Original weight}} \times 100 \quad (1)$$

$$\text{Yield (\%)} = \frac{\text{Actual yield}}{\text{Theoretical yield}} \times 100 \quad (2)$$

High-temperature carbonization ( $850^{\circ}\text{C}$ ) has a greater negative impact on the yield of samples with lower Rh. This likely happens because lower Rh samples have less pre-existing water content to drive out during carbonization. So, at high temperatures, they experience more severe decomposition and burn-off, leading to a sharper decrease in yield. Samples with higher Rh show a lesser decrease in yield at high temperatures. This could be due to pre-existing moisture in these samples, which acts as a buffer against excessive carbon burn-off at high temperatures. The water vaporization can also contribute to pore development, potentially slightly boosting the final yield. It is clear from this study that the final yield of activated carbon is significantly influenced by a number of factors, including moisture content, heating environment,

activation temperature, and Rh. It is essential to optimize these characteristics to produce high-quality activated carbon for particular uses.

### Features of the manufactured activated carbons

#### XRD analysis

Lower pyrolysis temperatures yield sharp XRD peaks at  $16^{\circ}$  and  $22^{\circ}$ , revealing the presence of crystalline cellulose, a hallmark of plant cell walls. But at  $850^{\circ}\text{C}$ , these peaks vanish, replaced by a broad one around  $22^{\circ}$ - $24^{\circ}$  as shown in Figure 2. This hints at the breakdown of cellulose and the formation of amorphous carbon, potentially with improved layer organization. While the pyrolysis temperature boosts the carbonization degree in both high and low relative humidity (RH)

samples, their behavior diverges at  $850^{\circ}\text{C}$ . High RH samples continue to carbonize, while those with low RH experience a decline. This suggests higher RH acts as a buffer, protecting against excessive decomposition at high temperatures due to its pre-existing moisture.

Increasing the activation temperature from  $650^{\circ}\text{C}$  to  $750^{\circ}\text{C}$  results in the emergence of "graphitic peaks" at  $31^{\circ}$  and  $51^{\circ}$ , even in samples activated at lower temperatures ( $650^{\circ}\text{C}$ ). These peaks provide valuable insights into the internal structure of the carbon, indicating a higher level of organization and crystallinity (Mai et al., 2019). The  $51^{\circ}$  peak, linked to the [101] plane, shines brighter in samples with higher humidity and at a scorching  $850^{\circ}\text{C}$ . This hints that extra moisture fuels the fire of localized graphitization. But at  $650^{\circ}\text{C}$  and  $750^{\circ}\text{C}$ , even with high humidity, these peaks are shier, whispering of a less organized, amorphous carbon structure compared to the  $850^{\circ}\text{C}$  high-five. Higher temperature and extra humidity team up to build and arrange these graphitic structures, as seen by the bolder peaks at  $31^{\circ}$  and  $51^{\circ}$ . Meanwhile, low-humidity samples generally prefer a messy life, with less crystallinity and more shapelessness, although some order might creep in at higher temperatures.

Peaks around  $1600$ -  $1400\text{ cm}^{-1}$  hint at C=O groups, affecting specific adsorption based on their polarity (Viswanathan et al., 2009). The broad peak at  $1050\text{ cm}^{-1}$  suggests diverse C-O bonds in ethers, alcohols, or phenols, potentially contributing to varied adsorption interactions (Angin, 2014). Activated carbon prepared with higher-moisture precursors exhibits a wider range and greater number of surface functional groups than those made with drier materials. This enhanced fingerprinting can be attributed to the influence of moisture content.

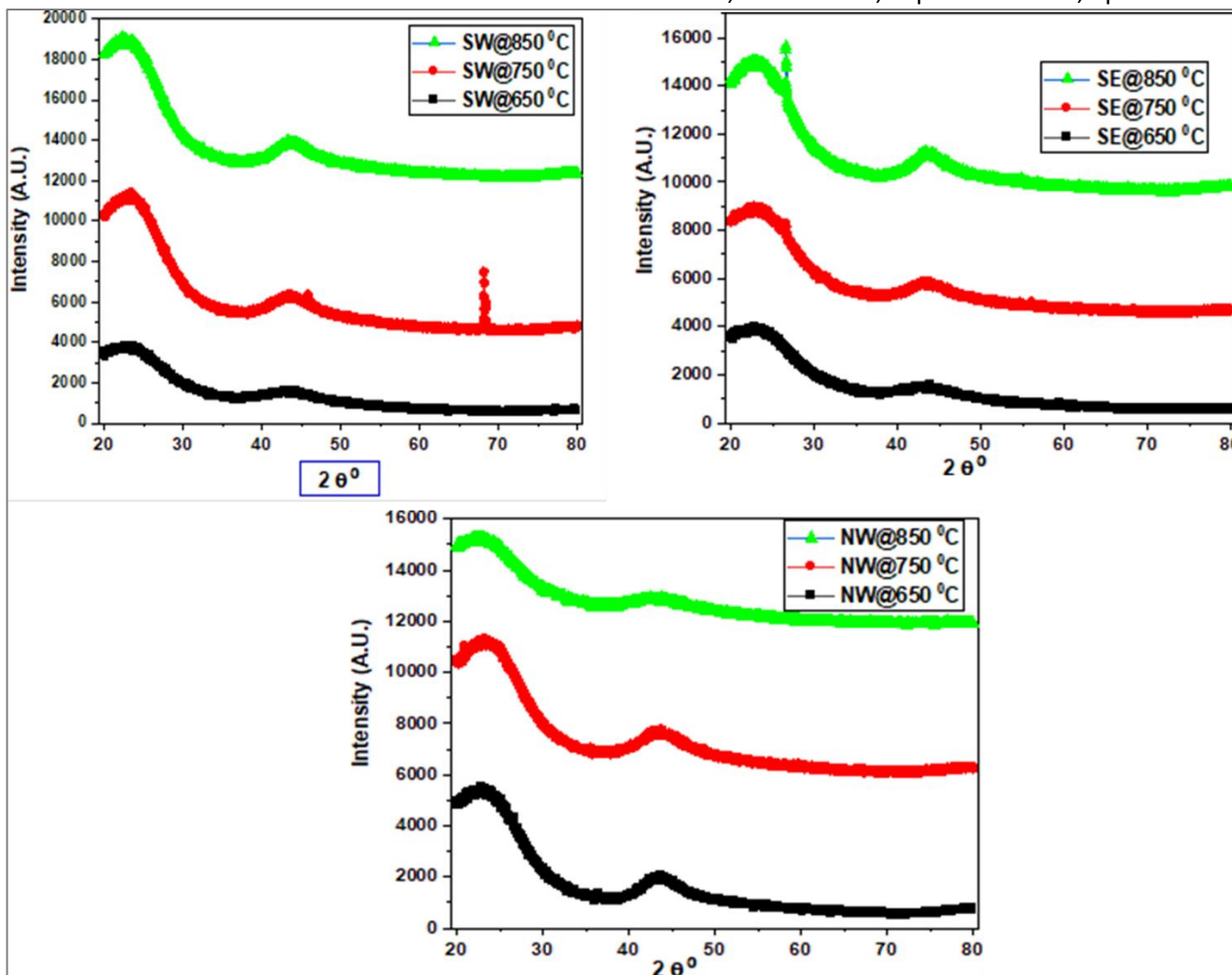


Figure 2. Activated carbon's X-ray diffraction pattern in samples with higher and lower humidity.

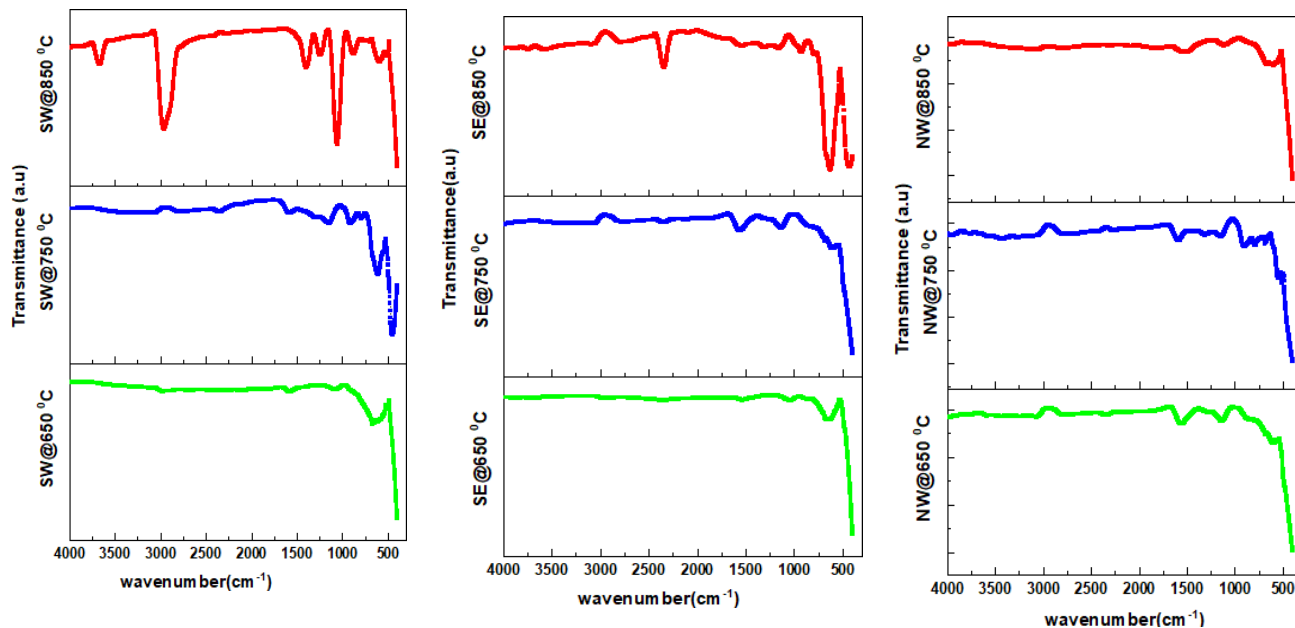


Figure 3. FTIR spectra of activated carbon with both samples from high humidity and lower humidity

*FTIR analysis*

This section examines the relationship between carbonization temperature and the relative humidity present in the precursor material and how these factors affect the formation of functional groups on activated carbon, which are essential to the material's adsorption capabilities. The influence of these variables is demonstrated by the FTIR spectra of activated carbons generated at various temperatures, shown in Figure 3. It was noticed that in the higher humidity sample, the broad peak around 3300 cm<sup>-1</sup> assigned to O-H stretching increases in intensity from 650 °C to 750 °C and then to 850 °C while that of lower humidity increases from 650 °C to 750 °C but sharply decreases at a higher temperature of 850 °C. The broad peak at 3300 cm<sup>-1</sup> indicates many -OH groups, crucial for polar interactions and adsorption. This confirms the increase in hydroxyl groups with increasing carbonization temperature (Rosli et al., 2023). The shoulder at 2925 cm<sup>-1</sup> suggests CH<sub>2</sub> and CH<sub>3</sub> groups, contributing to non-polar adsorption to a lesser extent.

*Raman spectroscopy analysis*

Raman spectroscopy is a powerful tool to confirm the presence of a carbon phase arising from localized graphitization during chemical treatment and carbonization. Where R, I<sub>D</sub>, and I<sub>G</sub> stand for the graphitization degree, the positioned D-peak intensity, and the positioned G-peak intensity, respectively.

The value of R was computed using Equation 3. Following computation, the value of R is approximately (0.84-0.87), indicating a somewhat higher index of graphitization (Liu et al., 2022). This technique can also reveal the resulting carbon structure's order or disorder (Abdelaal et al., 2023).

Figure 4 presents the vibrational fingerprint of coconut shell-activated carbon created in an oxygen-free environment at varying temperatures (650, 750, and 850 degrees Celsius) in the three zones of a wide relative humidity range. In Raman spectroscopy, the D band signifies the vibrational signature of disordered amorphous carbons, while the G band represents the regular vibrations of organized graphitic structures with sp<sup>2</sup> hybridization (Mondal et al., 2017), which are found 1600-1400cm<sup>-1</sup>, respectively. The D-band intensity divided by the G-band intensity (I<sub>D</sub>/I<sub>G</sub>), known as R, acts as a gauge for the level of graphitization and defect concentration in activated carbons (Karnan et al., 2016). While temperatures rise (650 to 850 °C), the R values unexpectedly drop (0.83 to 0.82), highlighting the potential dampening effect of lower moisture content on graphitization. Interestingly, the R values climb from 0.83 to 0.87 with increasing temperature, revealing a positive correlation between carbonization temperature and graphitization degree, facilitated by the higher moisture content of the humid sample.

$$R = \frac{I_D}{I_G} \tag{3}$$

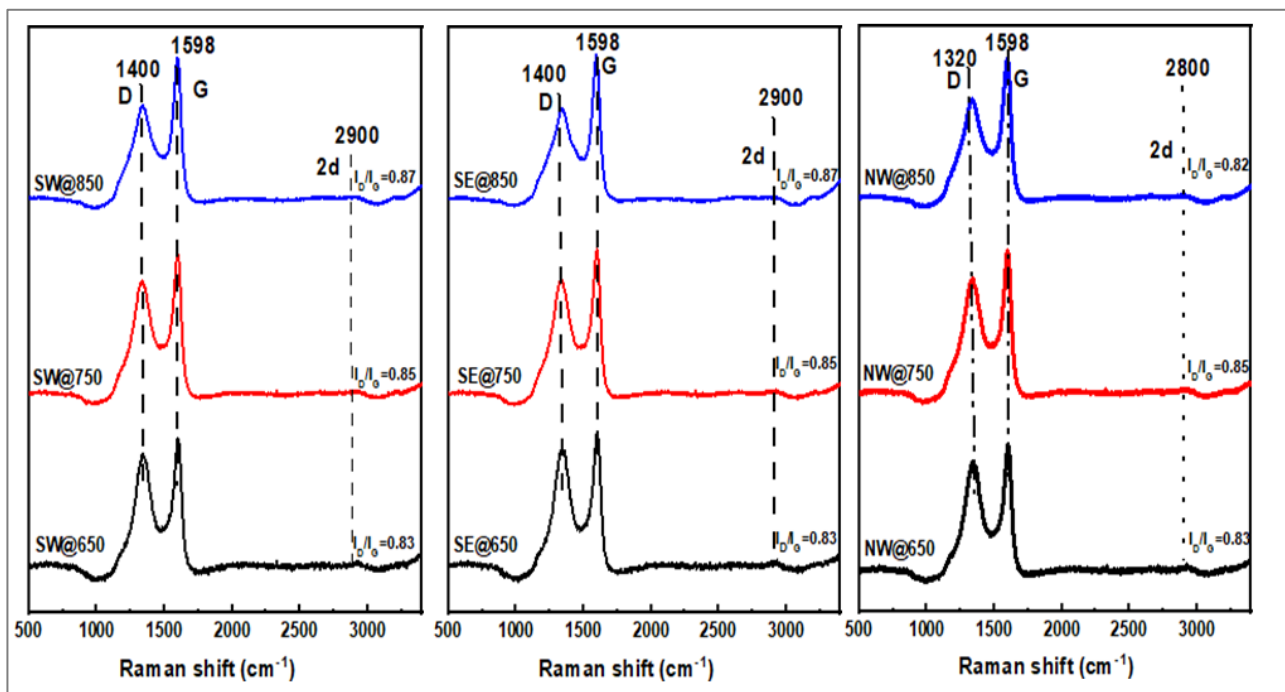
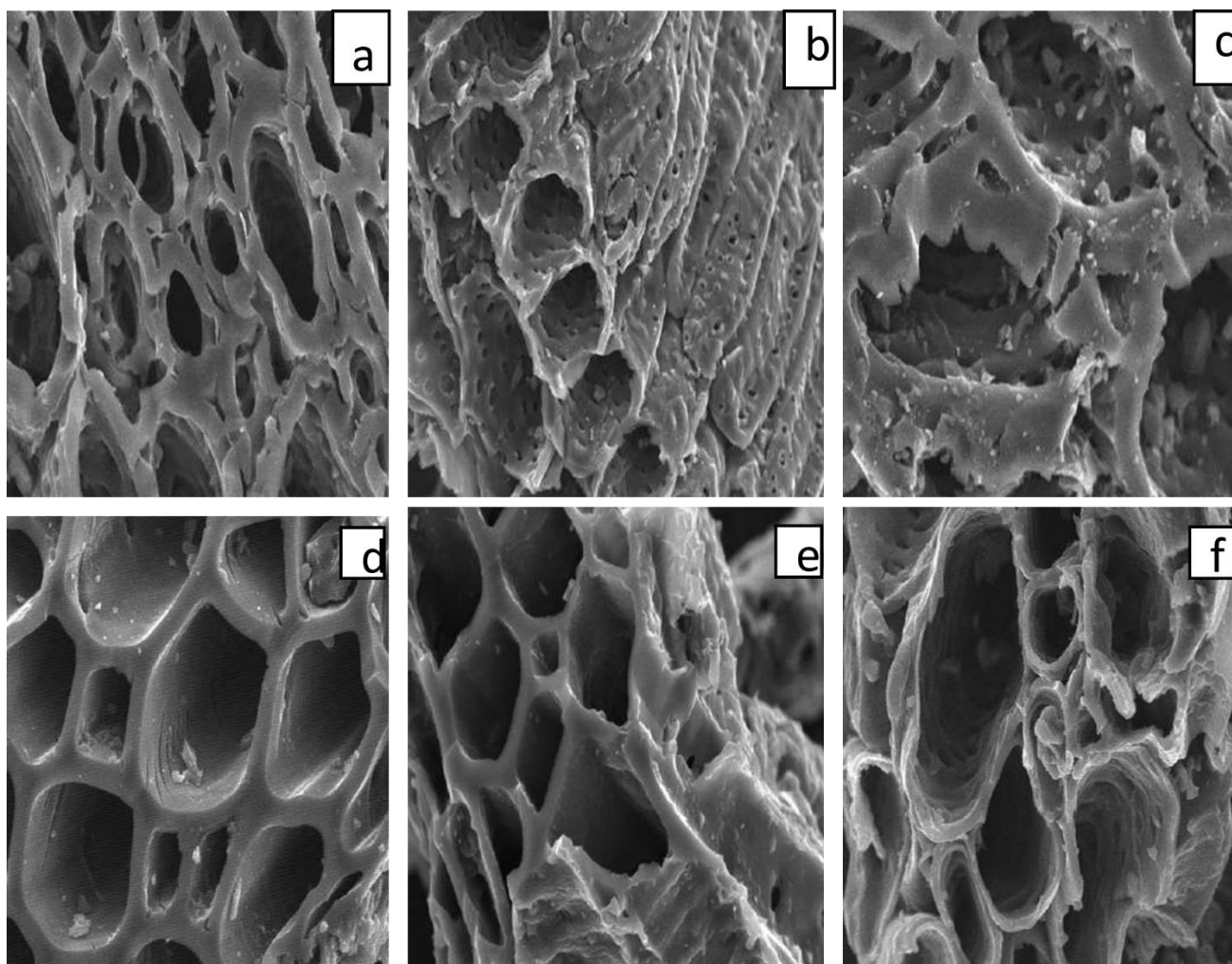


Figure 4. Pattern of activated carbon using Raman spectroscopy at 650, 750, and 850 degrees Celsius

*FESEM analysis*

Figure 5 shows pictures captured by a scanning electron microscope (FESEM) of activated carbon manufactured in an inert environment at different humidity and temperature levels. These images illustrate the changes in surface morphology at different activation temperatures: 650, 750, and 850 °C. By zooming in 10,000 times, we can observe how the activation

temperature and humidity influence the carbon's physical characteristics. This detailed analysis provides valuable insights into the intricate microstructure of the activated carbons, characterized by a diverse range of pore sizes and shapes and the material's potential for various applications, such as adsorption, catalysis, and energy storage (Rosli et al., 2023).



**Figure 5: FESEM images at 10,000 magnification**

The complex surface structures of activated carbon produced at varied temperatures (850°C) and humidity conditions (low and high) are revealed by the FESEM images shown in Figure 5. The North-West orientation is represented by each set of photographs (a, b, c), while the South-East and South-West viewpoints are shown in (d, e, f) at 10,000X.

The activated carbons' external surfaces transformed into intricate webs of pores thanks to a chemical exodus during carbonization. As these chemicals evaporated, they relinquished their former spaces, giving rise to a multitude

of pores of diverse sizes (Prahas et al., 2008; Kumar and Jena, (2016); Uçar et al., 2009).

Figure 5(a-c) showcases the surface morphology of activated carbon prepared in an inert atmosphere under low humidity conditions. Microscopy reveals a porous structure with diverse pore sizes and shapes. However, increasing the carbonization temperature to 860°C leads to a decrease in pore size and a more disintegrated microstructure (Köseoğlu & Akmil-Başar 2015). In contrast, activated carbon produced with higher humidity exhibits larger pores than drier samples and showcases a fascinating characteristic: these larger pores are not

haphazardly scattered but organized in a well-defined, structured manner.

BET surface area and pore size analysis were conducted on activated carbon synthesized at various relative

humidity levels and carbonization temperatures to delve deeper into the intricate pore characteristics observed. This quantitative analysis provides further confirmation and detailed insights into the pore structure.

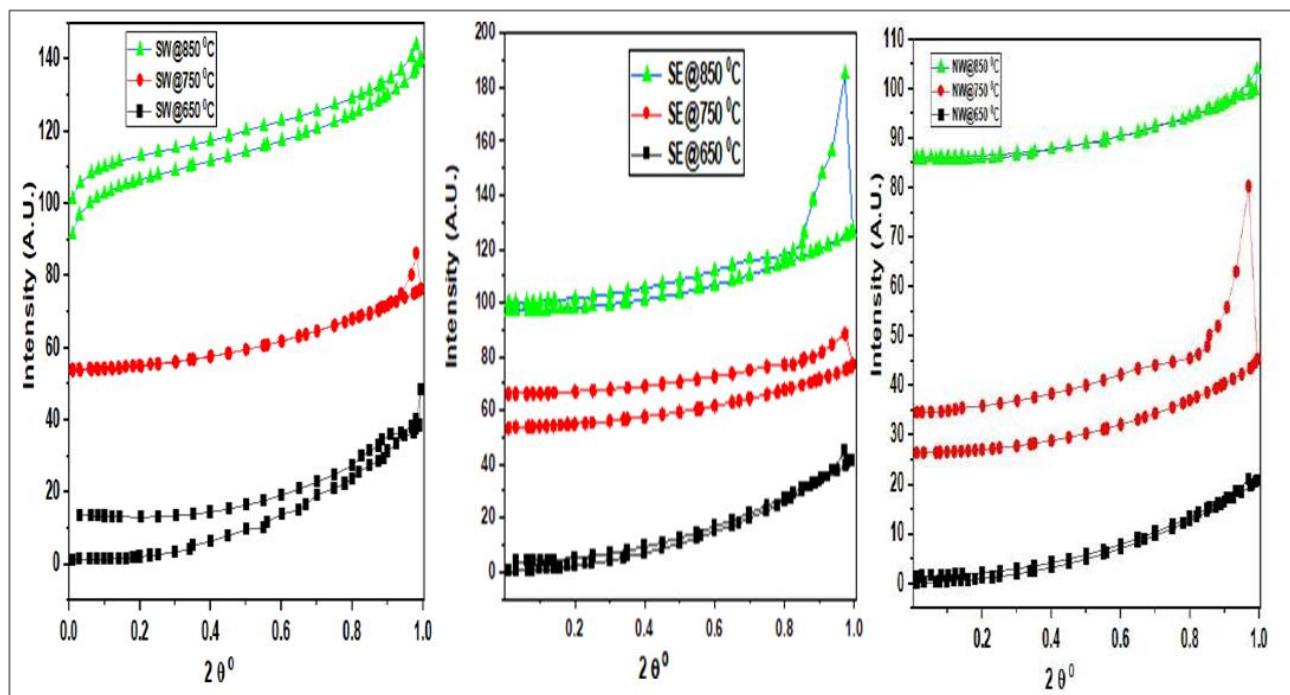


Figure 6 shows the nitrogen adsorption and desorption isotherm of activated cellulose nucifera produced in an inert atmosphere with different moisture content and activated temperature.

Table 1 The activated carbon's BET surface area and pore volume were measured in an inert atmosphere.

Samples	Surface area BET (m <sup>2</sup> / g)	Total pore Volume (cm <sup>3</sup> / g)	pore size (nm)	RH(%)
SW@650	2.9613	0.028040	37.87616	85
SW@750	5.0278	0.036424	28.97820	85
SW@850	9.6412	0.055780	23.14240	85
SE@650	1.8019	0.038731	85.97908	81
SE@650	9.5459	0.053506	22.42046	81
SE@850	13.3512	0.040369	12.09461	81
NW@650	2.3441	0.031074	53.02547	35
NW@750	2.7513	0.026366	38.33204	35
NW@850	0.2779	0.01777	255.93895	35

*BET surface and pore size analysis of the activated carbon.*

As illustrated in Figure 6, the nitrogen adsorption-desorption isotherms of these activated carbons tell an intriguing tale concealed inside their complex pore structure. Based on the classification system of the International Union of Pure and Applied Chemistry (IUPAC), they are reclassified as Type (I-IV) (Adinata et al., 2007). This type holds the key to understanding the exceptional adsorption potential of these materials. The consequence of this micropore magic is impressive high uptakes of nitrogen observed at these low pressures. This translates to the exceptional ability of these activated carbons to capture various gases, pollutants, and even liquids from their surroundings. Think of them as tiny vacuum cleaners, selectively grabbing unwanted molecules and holding them tight.

BET and FESEM analyses are crucial for characterizing activated carbon products providing data on total surface area, micro/mesopore volume and area, and pore size distribution (Sahu et al., 2020). The effects of relative humidity and activation temperature on the different properties of the activated carbon samples are shown in Table 1. This study shows that relative humidity and activation temperature synergistically influence porosity development in activated carbon samples. Raising the activation temperature over 650°C greatly increased the specific

surface area (micropore, mesopore, and BET surface area) and pore volume (micropore, mesopore, and total pore volume) in both low- and high-humidity settings. The activation process, which encourages the devolatilization of precursor carbon, enlargement of already-existing holes, and formation of new micro- and mesopores, is responsible for this trend that has been observed. (Köseoğlu & Akmil-Başar 2015); Hayashi et al., 2002); (Sun et al., 2010). The combined effects of relative density, moisture content, and activation temperature on the textural characteristics of activated carbon were examined in this work. Interestingly, different temperatures were ideal for optimizing pore volume and BET surface area depending on the precursor's initial relative density. Table 1 indicates that samples with a higher density reached their peak values at 850°C, while samples with a lower density reached their maximum at 750°C. The differences in moisture content in the precursors were the reason given for this mismatch. Increases in temperature above 750°C had a detrimental effect on pore volume and surface area in low-moisture samples. In the end, this enhanced porosity results in activated carbon with a higher capacity for adsorption and possible uses in a number of industries.

## CONCLUSION

Relative humidity emerged as a critical factor influencing activated carbon properties alongside established

parameters like temperature and impregnation. While higher humidity led to increased moisture content, it surprisingly boosted surface area for samples carbonized at higher temperatures. This study paves the way for optimizing activated carbon production from readily available coconut shells, considering humidity alongside traditional parameters, thereby paving the path for economical and diverse applications.

## FINANCE

For this work, the author did not get any funding.

## DISPUTE OF INTEREST

The authors certify that they have no competing interests.

## AUTHORS' CONTRIBUTION

A.I.I. Conceptualization, Methodology (Material Science Physicist), editing and Turnitin, N.C. Maduka

## NOVELTY OF THE WORK

Activated carbon production: This research looks beyond the standard practice and explores how varying RH levels impact surface area development in activated carbon derived from tall African coconut shells (*Cocos nucifera*) through pyrolysis.

Identifying the ideal pyrolysis temperature at various relative humidity levels: According to the study, the biomass's initial relative humidity (RH) determines the optimal temperature for maximizing surface area in the activated carbon. Higher pyrolysis temperature results in greater surface area for samples with a mid-range relative humidity (65-85%). Interestingly, the maximum surface area is reached at a particular temperature (750°C in this investigation) for samples with lower relative humidity.

This highlights the importance of considering RH as a factor influencing the activation process and tailoring the pyrolysis temperature to achieve optimal surface area in the final activated carbon product.

## REFERENCES

- Abdelaal, M. M., Hsu, H. H., Liao, W. L., Mohamed, S. G., Yang, C. C., & Hung, T. F. (2023). Hierarchical porous activated carbon anode for dual carbon lithium-ion capacitors: Energy storage mechanisms and electrochemical performances. *Journal of the Taiwan Institute of Chemical Engineers*, 104912. [Crossref].
- Adinata, D., Daud, W. M. A. W., & Aroua, M. K. (2007). Preparation and characterization of activated carbon from palm shell by chemical activation with K<sub>2</sub>CO<sub>3</sub>. *Bioresource technology*, 98(1), 145-149. [Crossref].



- Ajien, A., Idris, J., Md Sofwan, N., Husen, R., & Seli, H. (2023). Coconut shell and husk biochar: A review of production and activation technology, economic, financial aspect and application. *Waste Management & Research*, 41(1), 37-51. [\[Crossref\]](#).
- Amin, M., Chung, E., & Shah, H. H. (2023). Effect of different activation agents for activated carbon preparation through characterization and life cycle assessment. *International Journal of Environmental Science and Technology*, 20(7), 7645-7656. [\[Crossref\]](#)
- Angin, D. (2014). Production and characterization of activated carbon from sour cherry stones by zinc chloride. *Fuel*, 115, 804-811. [\[Crossref\]](#)
- Babu, B. (2024). Self-discharge in Rechargeable Electrochemical Energy Storage Devices. *Energy Storage Materials*, 103261. [\[Crossref\]](#)
- Foo, K. Y., & Hameed, B. H. (2012). Coconut husk derived activated carbon via microwave induced activation: effects of activation agents, preparation parameters and adsorption performance. *Chemical Engineering Journal*, 184, 57-65. [\[Crossref\]](#)
- Ghafoor, S., Nadeem, N., Zahid, M., & Zubair, U. (2024). Freestanding carbon-based hybrid anodes for flexible supercapacitors: Part I—An inclusive outlook on current collectors and configurations. *Wiley Interdisciplinary Reviews: Energy and Environment*, 13(2), e511. [\[Crossref\]](#)
- Hasdi, N. D., Ahmad, N., Ahya, M. K., & Puasa, S. W. (2023). An Overview of Activated Carbon Preparation from Various Precursors. *Scientific Research Journal*, 20(1), 51-87. [\[Crossref\]](#)
- Hayashi, J. I., Horikawa, T., Takeda, I., Muroyama, K., & Ani, F. N. (2002). Preparing activated carbon from various nutshells by chemical activation with K<sub>2</sub>CO<sub>3</sub>. *Carbon*, 40(13), 2381- 2386. [\[Crossref\]](#).
- Karnan, M., Subramani, K., Sudhan, N., Ilayaraja, N., & Sathish, M. (2016). Aloe vera derived activated high-surface-area carbon for flexible and high-energy supercapacitors. *ACS Applied Materials & Interfaces*, 8(51), 35191-35202. [\[Crossref\]](#)
- Köseoğlu, E., & Akmil-Başar, C. (2015). Preparation, structural evaluation, and adsorptive properties of activated carbon from agricultural waste biomass. *Advanced Powder Technology*, 26(3), 811-818. [\[Crossref\]](#).
- Kumar, A., & Jena, H. M. (2016). Preparation and characterization of high surface area activated carbon from Fox nut (*Euryale ferox*) shell by chemical activation with H<sub>3</sub>PO<sub>4</sub>. *Results in Physics*, 6, 651-658. [\[Crossref\]](#).
- Lan, J., Wang, B., Bo, C., Gong, B., & Ou, J. (2023). Progress on fabrication and application of activated carbon sphere in recent decade. *Journal of Industrial and Engineering Chemistry*. [\[Crossref\]](#)
- Liu, R., Yang, J., Liu, R., Tang, Y., Huang, L., & Shuai, Q. (2022). Effects of Nanopore Size on the Adsorption of Sulfamerazine from Aqueous Solution by  $\beta$ -Ketoenamine Covalent Organic Frameworks. *ACS Applied Nano Materials*, 5(12), 17851-17858. [\[Crossref\]](#)
- Mai, T. T., Vu, D. L., Huynh, D. C., Wu, N. L., & Le, A. T. (2019). Cost-effective porous carbon materials synthesized by carbonizing rice husk and K<sub>2</sub>CO<sub>3</sub> activation and their application for lithium-sulfur batteries. *Journal of Science: Advanced Materials and Devices*, 4(2), 223-229. [\[Crossref\]](#).
- Masthura, E., & Abdul, H. D. (2018). Effects of activation temperature on characteristics and microstructure of coconut shell-based activated carbon. *Eurasian J. Anal. Chem*, 4(13), 384-390.
- Mondal, A. K., Kretschmer, K., Zhao, Y., Liu, H., Fan, H., & Wang, G. (2017). Naturally nitrogen doped porous carbon derived from waste shrimp shells for high-performance lithium ion batteries and supercapacitors. *Microporous and Mesoporous Materials*, 246, 72-80. [\[Crossref\]](#)
- Oglou, R. C., Gokce, Y., Yagmur, E., & Aktas, Z. (2023). Production of demineralised high quality hierarchical activated carbon from lignite and determination of adsorption performance using methylene blue and p-nitrophenol: The role of surface functionality, accessible pore size and surface area. *Journal of Environmental Management*, 345, 118812. [\[Crossref\]](#)
- Platek-Mielczarek, A., Beda, A., Fic, K., & Ghimbeu, C. M. (2024). Synthesis and performance of binder-free porous carbon electrodes in electrochemical capacitors. *Journal of Materials Chemistry A*. [\[Crossref\]](#).
- Prahas, D., Kartika, Y., Indraswati, N., & Ismadji, S. J. C. E. J. (2008). Activated carbon from jackfruit peel waste by H<sub>3</sub>PO<sub>4</sub> chemical activation: Pore structure and surface chemistry characterization. *Chemical Engineering Journal*, 140(1-3), 32-42. [\[Crossref\]](#)
- Quan, C., Wang, H., Jia, X., & Gao, N. (2021). Effect of carbonization temperature on CO<sub>2</sub> adsorption behavior of activated coal char. *Journal of the Energy Institute*, 97, 92-99. [\[Crossref\]](#).
- Rosli, N. A., Ahmad, M. A., Noh, T. U., & Ahmad, N. A. (2023). Pineapple peel-derived carbon for adsorptive removal of dyes. *Materials Chemistry and Physics*, 128094. [\[Crossref\]](#)
- Sahu, A., Sen, S., & Mishra, S. C. (2020). Economical way of processing activated carbon from *Calotropis gigantea* and its suitability for application in Lithium/Sodium ion batteries. *Diamond and Related Materials*, 108, 107931. [\[Crossref\]](#)
- Sahu, A., Sen, S., & Mishra, S. C. (2023). A comparative study on characterizations of biomass derived activated carbons prepared by both normal and inert atmospheric heating conditions. *Journal of the Indian Chemical Society*, 100(4), 100943. [\[Crossref\]](#)

- Sun, Y., Wei, J., Wang, Y. S., Yang, G., & Zhang, J. P. (2010). Production of activated carbon by K<sub>2</sub>CO<sub>3</sub> activation treatment of cornstalk lignin and its performance in removing phenol and subsequent bioregeneration. *Environmental technology*, 31(1), 53-61. [\[Crossref\]](#).
- Uçar, S., Erdem, M., Tay, T., & Karagöz, S. (2009). Preparation and characterization of activated carbon produced from pomegranate seeds by ZnCl<sub>2</sub> activation. *Applied Surface Science*, 255(21), 8890-8896. [\[Crossref\]](#).
- Ulusal, A., Apaydın Varol, E., Bruckman, V. J., & Uzun, B. B. (2021). Opportunity for sustainable biomass valorization to produce biochar for improving soil characteristics. *Biomass Conversion and Biorefinery*, 11, 1041-1051. [\[Crossref\]](#)
- Viswanathan, B., Neel, P. I., & Varadarajan, T. K. (2009). Development of carbon materials forenergy and environmental applications. *Catalysis surveys from Asia*, 13, 164-183. [\[Crossref\]](#).
- Zhang, Z., Wang, P., Zhang, W., Hu, X., Zhang, X., Gou, Z., ... & Ding, X. (2024). A review: recent advances in conductive aerogels: assembly strategies, conductive mechanisms, influencing factors and applications. *Journal of Materials Science*, 1-30. [\[Crossref\]](#).
- Zhu, R., Yu, Q., Li, M., Zhao, H., Jin, S., Huang, Y., ... & Chen, J. (2021). Analysis of factors influencing pore structure development of agricultural and forestry waste-derived activated carbon for adsorption application in gas and liquid phases: A review. *Journal of Environmental Chemical Engineering*, 9(5), 105905. [\[Crossref\]](#)